JOURNAL OF GEOPHYSICAL RESEARCH, VOL. 112, D10S13, doi:10.1029/2006JD007725, 2007

Estimates of Cl atom concentrations and hydrocarbon kinetic reactivity in surface air at Appledore Island, Maine (USA), during International Consortium for Atmospheric Research on Transport and Transformation/Chemistry of Halogens at the Isles of Shoals

Alexander A. P. Pszenny,[1,2] Emily V. Fischer,[2,3] Rachel S. Russo,[1] Barkley C. Sive,[1] and Ruth K. Varner[1]

Received 30 June 2006; revised 23 October 2006; accepted 28 December 2006; published 3 May 2007.

[1] Average hydroxyl radical (OH) to chlorine atom (Cl·) ratios ranging from 45 to 119 were determined from variability-lifetime relationships for selected nonmethane hydrocarbons (NMHC) in surface air from six different transport sectors arriving at Appledore Island, Maine, during July 2004. Multiplying these ratios by an assumed average OH concentration of 2.5×10^6 cm^{-3} yielded estimates of Cl· concentrations of 2.2 to 5.6×10^4 cm^{-3}. Summed reaction rates of methane and more than 30 abundant NMHCs with OH and Cl· suggest that Cl· reactions increased the kinetic reactivity of hydrocarbons by 16% to 30% over that due to OH alone in air associated with the various transport sectors. Isoprene and other abundant biogenic alkenes were the most important hydrocarbon contributors after methane to overall kinetic reactivity.

Citation: Pszenny, A. A. P., E. V. Fischer, R. S. Russo, B. C. Sive, and R. K. Varner (2007), Estimates of Cl atom concentrations and hydrocarbon kinetic reactivity in surface air at Appledore Island, Maine (USA), during International Consortium for Atmospheric Research on Transport and Transformation/Chemistry of Halogens at the Isles of Shoals, *J. Geophys. Res.*, *112*, D10S13, doi:10.1029/2006JD007725.

1. Introduction

[2] Tropospheric ozone (O_3) plays a central role in regulating Earth's environment. Photolysis of O_3 in the presence of water vapor produces the OH radical, which is the principal oxidant for many important atmospheric compounds including methane (CH_4), other hydrocarbons, carbon monoxide (CO), nitrogen oxides (NO_X = NO + NO_2), and hydrochlorofluorocarbons. At the Earth's surface, high concentrations of O_3 can be toxic to humans and vegetation and it is one of the principal components of smog. In the middle and upper troposphere, O_3 is a major greenhouse gas. Until the 1970s it was thought that tropospheric O_3 was mainly supplied by transport from the stratosphere and removed by deposition involving reactions with organic materials at Earth's surface. Research since then has shown that tropospheric O_3 is in fact strongly affected by chemical production and loss within the troposphere.

[3] Chlorine radical chemistry influences O_3 in two ways [e.g., *Pszenny et al.*, 1993]. Some Cl· in marine air reacts directly with O_3 to initiate a catalytic destruction sequence:

$$\text{(R1)} \qquad Cl\cdot + O_3 \rightarrow ClO + O_2$$

$$\text{(R2)} \qquad ClO + HO_2 \rightarrow HOCl + O_2$$

$$\text{(R3)} \qquad HOCl + h\nu \rightarrow OH + Cl\cdot$$

[4] However, most Cl· reacts with hydrocarbons via hydrogen abstraction to form hydrogen chloride (HCl) vapor. The enhanced supply of odd-hydrogen radicals from hydrocarbon oxidation leads to O_3 production in the presence of sufficient NO_X. Thus chlorine radical chemistry represents a modest net sink for O_3 when the NO_X mixing ratio is less than about 20 pmol mol^{-1} and a net source of O_3 when NO_X mixing ratios are greater. Recent evidence from the Texas Air Quality Study indicates that chlorine radical chemistry in polluted coastal/urban air leads to significant net O_3 production [e.g., *Tanaka et al.*, 2000, 2003; *Riemer et al.*, 2002; *Chang et al.*, 2002].

[5] A major objective of the Chemistry of Halogens at the Isles of Shoals (CHAiOS) component of the International Consortium for Atmospheric Research on Transport and

[1]Institute for the Study of Earth, Oceans, and Space, University of New Hampshire, Durham, New Hampshire, USA.
[2]Mount Washington Observatory, North Conway, New Hampshire, USA.
[3]Now at Department of Atmospheric Sciences, University of Washington, Seattle, Washington, USA.

0148-0227/07/2006JD007725$09.00

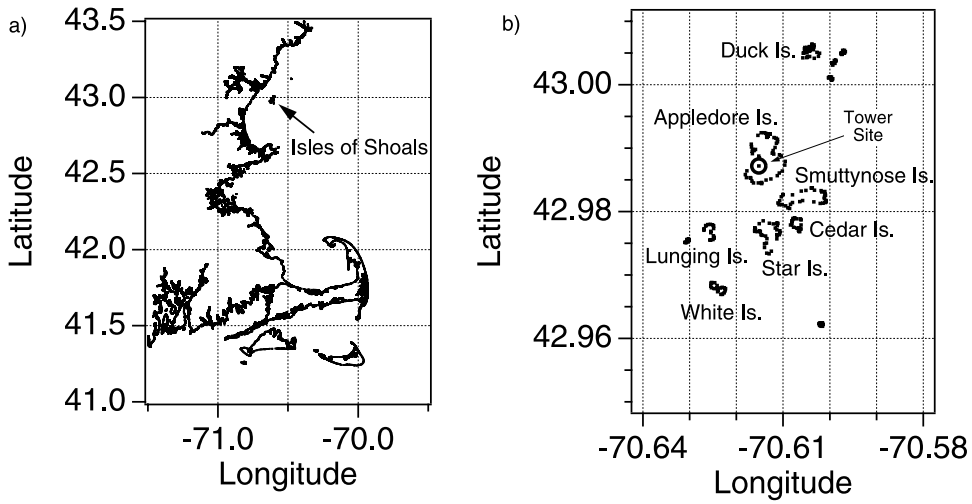

Figure 1. Map showing (a) the location of the Isles of Shoals on the New Hampshire–Maine, USA border, approximately 10 km offshore, and (b) location of the sampling site on Appledore Island.

Transformation (ICARTT) studies was to quantify the influences of halogen radicals on O_3 production/destruction in polluted air along the New England east coast during summer [*Fehsenfeld et al.*, 2006]. During the ICARTT/CHAiOS intensive sampling period in July and August 2004, a comprehensive suite of chemical and physical characteristics of near-surface air was quantified at an island site a few kilometers offshore from Portsmouth, New Hampshire, USA. In this paper, we estimate average [OH]/[Cl·] ratios from hydrocarbon variability-lifetime relationships and then evaluate the potential for chlorine radical chemistry to affect NMHC kinetic reactivity [*Carter*, 1991; *Seinfeld and Pandis*, 1998] due to OH attack. A discussion of the full implications of chlorine chemistry on the local/regional O_3 budget will be published separately once simulations of multiphase chemistry with a comprehensive model to be conducted by R. von Glasow (U. East Anglia) are completed.

2. Methods

2.1. Analytical Methods

[6] Hourly samples were collected in 2-liter electropolished stainless steel canisters (purchased from D.R. Blake, University of California, Irvine) from 2 to 29 July 2004 through an inlet at 43 m ASL on the roof of a WWII-era surveillance tower on Appledore Island, Maine (42°59′13.5″N, 70°23′55.4″W, ~0.39 km^2), located approximately 10 km off the shore of New Hampshire (Figure 1). Canister samples were pressurized to 35 psig using a single-head metal bellows pump (MB-302MOD, Senior Flexonics, Sharon, Massachusetts) and returned to the University of New Hampshire every four days for determination of C_2–C_{10} NMHCs, C_1–C_2 halocarbons, C_1–C_5 alkyl nitrates and selected organic sulfur compounds by gas chromatography using a three-GC system equipped with two electron capture detectors (ECDs), two flame ionization detectors (FIDs) and one mass spectrometer (MS). The samples were analyzed by cryotrapping 1772 cm^{-3} STP (273 K, 1 atm) of air on a glass bead filled loop immersed in liquid nitrogen. After each sample was trapped, the loop was isolated, warmed to 80°C and the sample was injected. Helium carrier gas flushed the contents of the loop and the stream was split into five substreams, each feeding a separate GC column. One 30 m × 0.53 mm I.D., 10 μm film thickness CP-Al_2O_3/Na_2SO_4 PLOT column (Varian, Inc., Walnut Creek, California), one 60 m × 0.25 mm I.D., 1 μm film thickness OV-1701 column (Ohio Valley, Marietta, Ohio), one 60 m × 0.32 mm I.D., 1.0 μm film thickness DB-1 column (J&W Scientific, Folsom, California), and two 60 m × 0.25 mm I.D., 1.4 μm film thickness OV-624 columns (Ohio Valley, Marietta, Ohio) were used for the trace gas separation. One of the OV-624 columns and the OV-1701 were plumbed into ECDs and used for measuring the halocarbons and alkyl nitrates (not discussed in this paper). The PLOT and DB-1 columns were connected to FIDs and used for the C_2–C_{10} NMHC quantification. The second OV-624 column provided separation for the MS. Electron impact mode for the MS was used for sample ionization along with single ion monitoring. This system provided duplicate measurements for numerous halocarbons and NMHCs. Finally, the gas separation was unique for each of the columns and thus any gases coeluting on one column were usually resolved on another. For the standard analysis protocol, a 1772 cm^{-3} STP aliquot from one of two working standards was assayed every ninth analysis, thereby quickly drawing attention to any drift or malfunction of the analytical system. The measurement precision for individual halocarbons, hydrocarbons, and alkyl nitrates ranged from 0.1 to 12% depending on the compound and mixing ratio. Further details of the NMHC sampling and analysis are given by *Sive et al.* [2005], *Zhou et al.* [2005], and Y. Zhou et al. (Bromoform and dibromomethane measurements in the seacoast region of New Hampshire, 2002–2004, submitted to *Journal of Geophysical Research*, 2006).

2.2. Transport Sector Classification and Local Meteorology

[7] Samples were classified by source region (Figure 2) using back trajectories and the corresponding column and

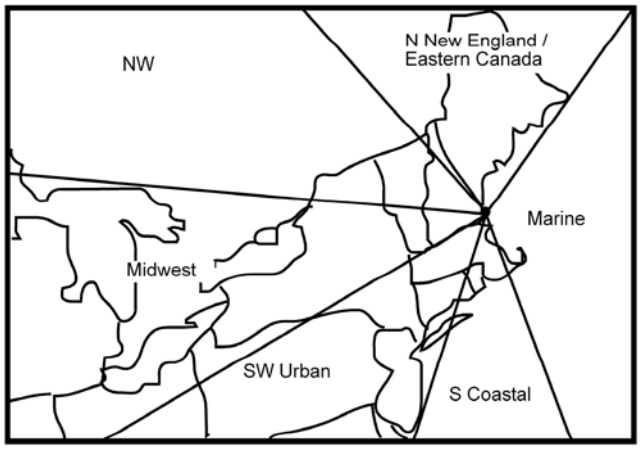

Figure 2. Idealized depiction of the six transport sectors into which sampled air was classified. Details of the classification scheme are given by *Fischer et al.* [2006].

footprint residence time components of retroplumes [*Fischer et al.*, 2006]. Column residence time and footprint residence plots provided by the NOAA Chemical Sciences Division (http://esrl.noaa.gov/csd/ICARTT/analysis/) and HYSPLIT trajectories archived at Plymouth State University (http://pscwx.plymouth.edu/ICARTT/archive.html) were visually inspected to create six regional flow regime classifications. To generate the column residence time and footprint residence plots, the particle dispersion model FLEXPART [*Stohl et al.*, 1998, 2005] was run in backward mode [*Stohl et al.*, 2003; *Seibert and Frank*, 2004] in order to see where the sampled air masses were potentially exposed to emissions. FLEXPART was driven with ECMWF analyses of 0.36° resolution and accounts for turbulence and deep convection, in addition to the transport by grid-resolved winds. Every 3 hours, 40000 particles were released from the location of the measurement site and followed backward in time for 20 days to calculate a so-called potential emission sensitivity (PES) function, as described by *Seibert and Frank* [2004] and *Stohl et al.* [2003]. For the emission distribution, the inventory of *Frost et al.* [2006] with a base resolution of 4 km, remapped to the 0.25° × 0.333° resolution of the PES output, was used [*Frost et al.*, 2006].

[8] The HYSPLIT trajectories [*Draxler and Rolph*, 2005] were initialized from 10, 500, and 1000 meters above ground level every 6 hours using the North American Mesoscale (NAM) 12 km analysis. Over-water transit times from the coast to Appledore Island were estimated using 36-hour back trajectories calculated from the NOAA ESRL profiler network and ocean buoy data (http://www.etl.noaa.gov/data/profiler_data/processed/ProfilerTrajectory/). Local meteorological data were obtained from National Oceanic and Atmospheric Administration (NOAA) meteorological station IOSN3 on White Island, approximately 2.5 km south of Appledore Island.

2.3. Computational Methods

[9] The basis for the [OH]/[Cl·] ratio estimates is the coherent variability-lifetime trends exhibited by compounds with similar atmospheric source-sink distributions. Both measurements [e.g., *Ehhalt et al.*, 1998; *Jobson et al.*, 1998, 1999, 2004; *Millet et al.*, 2004] and modeling studies [e.g., *Hamrud*, 1983; *Ehhalt et al.*, 1998; *Lenschow and Gurarrie*, 2002] indicate that appropriately selected sets of compounds follow power law relationships

$$S_{\ln X} = A\tau^{-b} \tag{1}$$

where $S_{\ln X}$ is the standard deviation of the natural logarithms of a time series of measured mixing ratios, τ is the local lifetime of the compound (defined below), and A and b are fit parameters. Physical meaning can be attached to parameter A if it is assumed that the measurements represent air parcels with the same initial mixing ratios but varying transit times. Equation (1) can then be rewritten as

$$S_{\ln X} = A\tau^{-b} = (\Psi/\tau)^{b} \tag{2}$$

where Ψ is related to some measure of the distribution of transit times from sources [*Jobson et al.*, 1999]. Smaller values of Ψ imply shorter source-receptor transit times. Parameter b ranges between 0 and 1 and can be interpreted as a measure of source-receptor distances [*Jobson et al.*, 1998, 1999]. Smaller values tend to result from observations made close to sources, where variability is driven by source strength variations, while larger values tend to result from observations far from sources and after chemical losses have occurred.

[10] In polluted air, motor vehicles are the dominant source of many C_3 to C_8 aliphatic and C_6 to C_9 aromatic hydrocarbons. The dominant sink for these compounds is usually oxidation initiated by OH. If it is assumed that reaction with OH is the only sink then the local lifetime of a compound is

$$\tau = 1/(k_{OH} \cdot [OH]) \tag{3}$$

where k_{OH} is the compound's OH reaction rate coefficient. Assuming reaction with Cl· to be an additional sink alters (3) to

$$\tau = 1/\{(k_{OH} \cdot [OH]) + (k_{Cl} \cdot [Cl\cdot])\}. \tag{4}$$

[11] Varying [Cl·] relative to [OH] in (4) to minimize the residuals of a fit to (1) yields a "best" estimate of [OH]/[Cl·]. The optimizations were done in two steps. In Excel (Version 11.2.5 for Mac) an approximate maximum correlation of log-transformed values of $S_{\ln X}$ and τ was obtained by varying [Cl] manually from an inconsequential value (500 cm^{-3}) to a value higher than can reasonably be expected in polluted MBL air (10^6 cm^{-3}). For all six transport subsets this yielded a relation with a single maximum in the correlation coefficient for [Cl] between 2 and 6×10^4 cm^{-3}. Excel's "solver" tool was then used to automatically home in on the [Cl] value that maximized the correlation coefficient for each subset. The OH concentration was held fixed at 2.5×10^6 cm^{-3} on the basis of *Warneke et al.* [2004] who estimated average [OH] in surface air encountered by NOAA Ship *Ronald H. Brown* within an approximately 100 km × 100 km area surrounding Appledore Island from mid-July to early August 2002

Table 1. Rate Coefficients at 298 K Used for Reactions of CO and Hydrocarbons With OH and Cl Atoms

Compound	k_{OH}, cm^{-3} $molecule^{-1}$ s^{-1}	Reference	k_{Cl}, cm^{-3} $molecule^{-1}$ s^{-1}	Reference
Carbon monoxide	1.50×10^{-13}	*DeMore et al.* [1997]	3.15×10^{-14}	*DeMore et al.* [1997]
Methane	6.40×10^{-15}	*Atkinson et al.* [2005]	1.00×10^{-13}	*Atkinson et al.* [2005]
Ethane	2.40×10^{-13}	*Atkinson et al.* [2005]	5.90×10^{-11}	*Atkinson et al.* [2005]
Ethene	9.00×10^{-12}	*Atkinson et al.* [2005]	1.10×10^{-10}	*Atkinson et al.* [2005]
Ethyne	9.00×10^{-13}	*Atkinson* [1990]	5.20×10^{-11}	*Atkinson et al.* [2005]
Propane	1.10×10^{-12}	*Atkinson et al.* [2005]	1.40×10^{-10}	*Atkinson et al.* [2005]
Propene	3.00×10^{-11}	*Atkinson et al.* [2005]	2.70×10^{-10}	*Atkinson et al.* [2005]
i-butane	2.12×10^{-12}	*Atkinson* [2003]	1.43×10^{-10}	*Atkinson* [1997]
n-butane	2.36×10^{-12}	*Atkinson* [2003]	2.18×10^{-10}	*Atkinson* [1997]
t-2-butene	6.40×10^{-11}	*Atkinson* [1997]	3.31×10^{-10}	*Ezell et al.* [2002]
1-butene	3.14×10^{-11}	*Atkinson* [1997]	3.38×10^{-10}	*Ezell et al.* [2002]
c-2-butene	5.64×10^{-11}	*Atkinson* [1997]	3.76×10^{-10}	*Ezell et al.* [2002]
i-pentane	3.60×10^{-12}	*Atkinson* [2003]	2.20×10^{-10}	*Atkinson* [1997]
n-pentane	3.80×10^{-12}	*Atkinson* [2003]	2.80×10^{-10}	*Atkinson* [1997]
2-methyl-2-butene	8.69×10^{-11}	*Atkinson* [1997]	3.95×10^{-10}	*Ezell et al.* [2002]
1-pentene	3.14×10^{-11}	*Atkinson* [1997]	3.97×10^{-10}	*Ezell et al.* [2002]
Cyclohexane	6.97×10^{-12}	*Atkinson* [2003]	3.50×10^{-10}	*Atkinson* [1997]
2-methylpentane	5.20×10^{-12}	*Atkinson* [2003]	2.90×10^{-10}	*Atkinson* [1997]
3-methylpentane	5.20×10^{-12}	*Atkinson* [2003]	2.80×10^{-10}	*Atkinson* [1997]
n-hexane	5.20×10^{-12}	*Atkinson* [2003]	3.40×10^{-10}	*Atkinson* [1997]
n-heptane	6.76×10^{-12}	*Atkinson* [2003]	3.97×10^{-10}	*Ezell et al.* [2002]
n-octane	8.11×10^{-12}	*Atkinson* [2003]	4.60×10^{-10}	*Atkinson* [1997]
n-nonane	9.70×10^{-12}	*Atkinson* [2003]	4.80×10^{-10}	*Atkinson* [1997]
n-decane	1.10×10^{-11}	*Atkinson* [2003]	5.50×10^{-10}	*Atkinson* [1997]
Isoprene	1.00×10^{-10}	*Atkinson et al.* [2005]	5.10×10^{-10}	*Finlayson-Pitts et al.* [1999]
2,4-dimethylpentane	4.80×10^{-12}	*Atkinson* [2003]	2.90×10^{-10}	*Atkinson* [1997]
Methylcyclohexane	9.60×10^{-12}	*Atkinson* [2003]	3.90×10^{-10}	*Atkinson* [1997]
2,2,4-trimethylpentane	3.34×10^{-12}	*Atkinson* [2003]	2.60×10^{-10}	*Atkinson* [1997]
Benzene	1.23×10^{-12}	*Atkinson* [1990]	4.00×10^{-12}	*Wallington et al.* [1988]
Toluene	5.96×10^{-12}	*Atkinson* [1990]	5.90×10^{-11}	*Shi and Bernhard* [1997]
1,3,5-trimethylbenzene	5.67×10^{-11}	*Atkinson* [1990]	2.42×10^{-10}	*Wang et al.* [2005]
a-pinene	5.30×10^{-11}	*Atkinson et al.* [2005]	5.30×10^{-10}	*Timerghazin and Ariya* [2001]
b-pinene	7.90×10^{-11}	*Atkinson* [1997]	5.30×10^{-10}	*Finlayson-Pitts et al.* [1999]
Limonene	1.70×10^{-10}	*Atkinson* [1997]	6.40×10^{-10}	*Finlayson-Pitts et al.* [1999]

using a "full" source-sink calculation and, separately, the parameterization of *Ehhalt and Rohrer* [2000]. Substituting k_{Cl} and [Cl] for their ozone analogs in equation (26) of *Ehhalt et al.* [1998] gives:

$$\tau^{-1} = k_{OH}[OH] + k_{Cl}[Cl] = k'[OH] \quad (5)$$

where k' is a fictitious rate constant determined from the fit of S_{lnX} versus τ. Rearranging (5) yields

$$k_{Cl}/(k' - k_{OH}) = [OH]/[Cl], \quad (6)$$

which shows that calculated [Cl] scales directly with assumed [OH]. *Jobson et al.* [1999] described and used an analogous fitting method to estimate relative radical abundances during polar sunrise at Alert, NWT, Canada.

3. Results and Discussion

3.1. Variability-Lifetime Relationship Calculations

[12] A subset of eight NMHCs (ethyne, propane, i-butane, n-butane, i-pentane, n-pentane, benzene and toluene) was selected with which to construct variability-lifetime relationships and estimate [OH]/[Cl·] as described above. The selection criteria were (1) similar source distributions (specifically, dominated by motor vehicle emissions), (2) small percentage (<3%) of values below detection limit to keep bias in variability small, (3) lifetimes against reaction with 2.5×10^6 OH cm^{-3} between ~0.5 and ~4 days (at 298 K), (4) lifetimes against reaction with a preliminary estimate of ~4×10^4 Cl· cm^{-3} [*Goldan et al.*, 2005; *Keene et al.*, 2007] of ~0.5 day or longer, and (5) negligible reaction rates with oxidants other than OH and Cl·. Criteria 3 and 4 reduce potential confounding effects of compounds with highly variable sources and sinks (e.g., alkenes) and of long-lived compounds whose variability may be affected substantially by multiple sources (e.g., ethane). Rate coefficients used are given in Table 1. Mixing ratios of these eight NMHCs and those of O_3 and CO for sample subsets associated with each of the six transport sectors are summarized in Figure 3.

3.2. Interpretation of Relationships

[13] The results of fits to equation (1) are given in Table 2 and illustrated in Figure 4. Two groups of relationships are clearly evident in Figure 4. One group contains the sample subsets associated with the three "westerly" transport sectors (SW urban, midwest and NW) while the other group contains the subsets associated with "easterly" transport sectors. This grouping is reflected in the values of the transit time variability index (Ψ) derived from fit parameter A (Table 2). Less transit time variability for the "westerly" group is consistent with the shorter upwind distances to shore (10 to 50 km) and shorter transit times from major

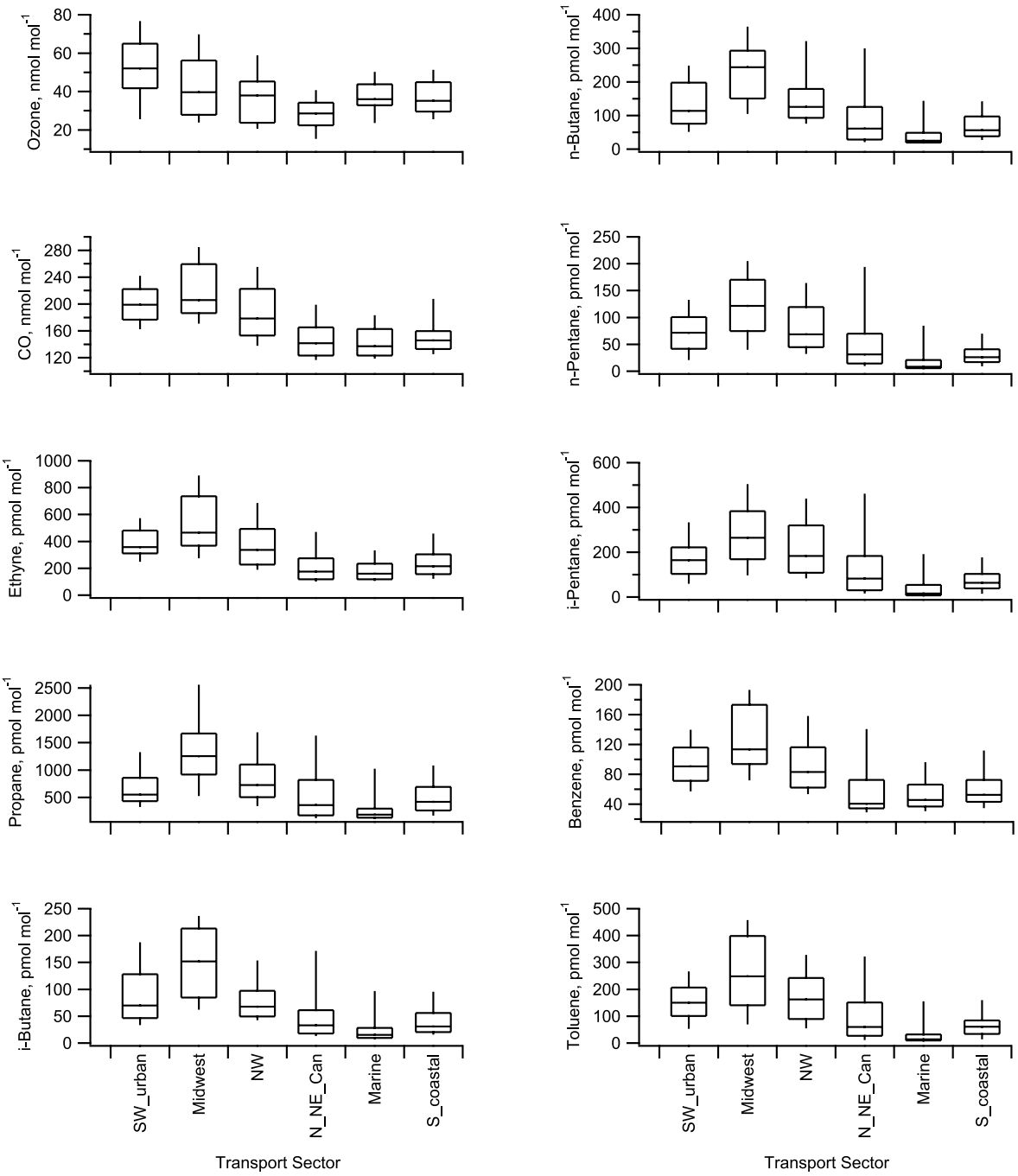

Figure 3. Box-whisker plot summaries by transport sector of the measured mixing ratios of CO, O_3 and the eight NMHCs used in constructing variability-lifetime relationships from which [OH]/[Cl·] ratios were estimated. The central line across each box indicates the median; the top and bottom of each box indicate the 75th and 25th percentile values, respectively; and the upper and lower whisker ends indicate the 90th and 10th percentile values, respectively.

sources of vehicular emissions than for the "easterly" group. The value of A is sensitive to the assumed value of [OH] and the estimated value of [Cl·] so some caution is necessary in interpreting the absolute values of Ψ.

[14] The values of parameter b vary with transport sector in a different but somewhat consistent manner as that described above for parameter A (Table 2). The three smallest values, suggesting relative proximity to sources of the selected NMHCs, are associated with the three "westerly" transport sectors. The value for the SW urban sector is larger than those for the midwest and NW sectors, possibly because of influence of intense emissions from New York City and other Eastern Seaboard metropolitan areas. Relationships for the two "easterly" sectors that cover the relatively heavily populated New England coastline have b values similar to that for the SW urban sector.

Table 2. Results of Fits to Functions of the Form $S_{lnX} = A\tau^{-b}$ by Transport Sector for [OH] = 2.5×10^6 molecules cm^{-3}

Transport Sector	N	A	ΔA[a]	b	Δb[a]	Ψ,[b] hours	[OH]/[Cl] From Fit	"Best" [Cl],[c] molecules cm^{-3}
SW urban	82	0.544	0.048	0.34	0.16	4.1 (0.5–11)	53	$4.7 \pm 0.12 \times 10^4$
Midwest	69	0.554	0.068	0.20	0.20	1.2 (~0–7.3)	119	$2.1 \pm 0.060 \times 10^4$
NW	120	0.589	0.062	0.23	0.17	2.3 (~0–8.2)	45	$5.6 \pm 0.15 \times 10^4$
N_NE_Canada	168	0.951	0.095	0.37	0.19	21 (10–31)	64	$3.9 \pm 0.13 \times 10^4$
Marine	78	0.918	0.134	0.54	0.31	20 (8.3–30)	77	$3.3 \pm 0.083 \times 10^4$
S Coastal	123	0.826	0.085	0.41	0.20	15 (5.8–21)	112	$2.2 \pm 0.087 \times 10^4$

[a]95% confidence interval for value in preceding column.
[b]$\Psi = A^{1/b} \times 24$; range (in parentheses) corresponds to extremes calculated using $A \pm \Delta A$ and $b \pm \Delta b$.
[c]Uncertainties are approximate 95% confidence intervals; see text for explanation.

The marine sector relationship shows the largest b value, consistent with relatively long source-receptor distances and transit over ocean areas where emissions of the selected NMHCs are much less than emissions over land.

3.3. Estimates of [OH]/[Cl·] Ratios and Cl· Concentrations

[15] Also given in Table 2 are the average [OH]/[Cl·] ratios estimated from the power law fits and the average Cl· concentrations calculated from those ratios assuming [OH] = 2.5×10^6 molecules cm^{-3}. Because [OH] is assumed constant and [OH]/[Cl·] is also constant the only source of uncertainty in calculated [Cl·] derives from uncertainties in the rate constants used for the 16 reactions involved. This uncertainty has a potential systematic component due to the assumption of atmospheric conditions of 298 K, 1 atm and a nonsystematic component due to variability in laboratory rate constant determinations. Using 285 K, 0.8 atm (an approximation for average conditions at 2 km altitude) increases calculated [Cl·] by 6% to 13% depending on transport sector. To estimate uncertainties due to variability in laboratory rate constant determinations, optimizations were repeated 25 times for each transport sector subset, each time with all 16 rate constants varied randomly within the uncertainty ranges given for them in the respective source references. Tabulated uncertainties in [Cl·] are approximate 95% confidence limits based on these 25 optimization runs.

[16] The [Cl·] do not group in a straightforward manner like the fit parameters. Two possible explanations are (1) [Cl·] was high in SW urban sector air because average local surface wind speeds were more than twice those for other sectors and sea salt aerosol concentrations and fluxes were correspondingly greater [*Keene et al.*, 2007] and (2) [OH] was lower than 2.5×10^6 molecules cm^{-3} in NW sector air, which tended to be cooler and dryer than air from other sectors. Modeling is in progress that may eventually allow resolution of this incongruity.

[17] Published estimates of [Cl·] for various locations and times are presented in Table 3. Because direct measurement of Cl· in ambient air is not yet technologically possible, all existing estimates are based on measurements of hypothesized Cl· precursors or reactant species in combination with a variety of modeling techniques ranging in complexity from straightforward hydrocarbon ratio methods [e.g., *Jobson et al.*, 1994] to detailed multiphase chemistry models [e.g., *Sander and Crutzen*, 1996]. The [Cl·] concentrations of a few $\times 10^4$ cm^{-3} estimated in this study are well within the range of previous estimates, which spans more than four orders of magnitude. No two published studies have employed exactly the same method/model combination, rendering quantitative comparisons questionable, even within the subgroups of studies identified in Table 3.

[18] We are aware of only one previous estimate of [OH]/[Cl·]. Using a technique analogous to the one employed in the present study in which a fixed concentration of Cl atoms was assumed, *Jobson et al.* [1999] estimated relative abundances of [OH]:[Cl·]:[Br·] of ~17:1:3300 in surface air at an ice floe location near Alert NWT during polar sunrise. Previous work at Alert had strongly suggested an important role of Cl and Br chemistry during low-ozone events observed around the time of polar sunrise [*Jobson et al.*, 1994].

3.4. NMHC Kinetic Reactivity With OH and Cl·

[19] Incremental reactivity (IR) is an index of the influence of a volatile organic compound (VOC) on ozone

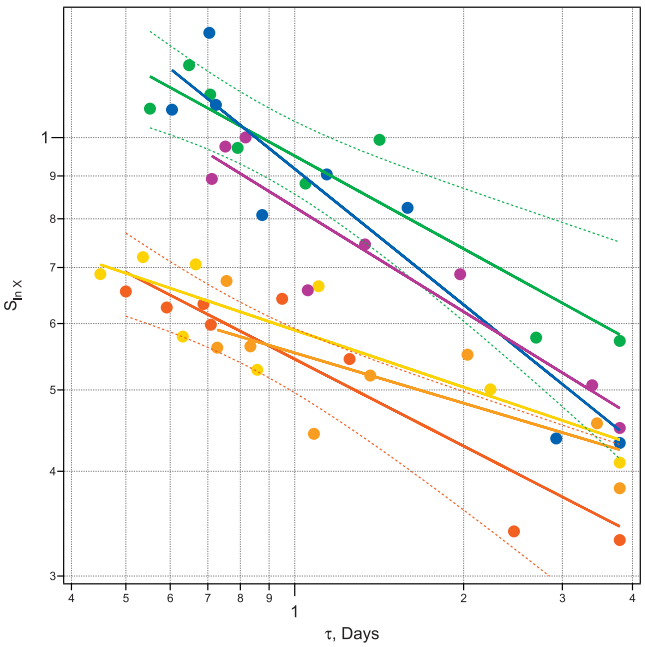

Figure 4. Plots of S_{lnX} versus τ for the eight selected NMHC and best fit variability-lifetime relationships (solid lines) for the subsets of canister samples representing the six transport sectors defined by *Fischer et al.* [2006]. Colors represent sectors as follows: red, SW urban; orange, midwest; yellow, NW; green, north-northeast Canada; blue, marine; and violet, south coastal. Dotted lines illustrate 95% confidence intervals for two of the six fits. Numerical fit results are given in Table 2.

Table 3. Estimates of Tropospheric [Cl·] From Various Studies

[Cl·], 10^4 cm^{-3}	Location, Time	Reference; Notes
	Inferred From MBL NMHC Measurements	
<1	California coast, spring	*Parrish et al.* [1992]
1–10	Alert, NWT, sunrise	*Jobson et al.* [1994]
3–7	SE N. Atlantic, summer	*Wingenter et al.* [1996]
4–76	equatorial N. Pacific, boreal autumn	*Singh et al.* [1996a]
<0.7	N. Atlantic/Med., spring	*Rudolph et al.* [1997]
~0.7	Southern Ocean, summer	*Wingenter et al.* [1999]
2–6	Appledore Island, summer	this study
	Inferred From Global Budgets of C_2Cl_4	
<0.1–1	global MBL	*Rudolph et al.* [1996]
<0.5–3	global MBL (daytime)	*Singh et al.* [1996b]
	Inferred From Models	
0.1	global troposphere	*Singh and Kasting* [1988]; HCl (1 nmol mol^{-1}) + OH
10–100	N. Atlantic, summer	*Keene et al.* [1990]; Cl_2 from aerosol Cl^- deficit data
<1–10	coastal Florida (Miami), winter	*Pszenny et al.* [1993]; HCl and other inorganic Cl gas data
<0.1–1	polluted MBL	*Sander and Crutzen* [1996]; MOCCA
1–10	remote MBL	*Vogt et al.* [1996]; MOCCA
0.7/1.8	remote/polluted MBL	*Keene et al.* [1998]; MOCCA
~0.2	Oahu, Hawaii, September	*Pszenny et al.* [2004]; MOCCA

Table 4a. Percentage Contributions of OH and Cl Reactions to Kinetic Reactivities of Compounds Calculated Using the Median Mixing Ratios of the Respective Compounds in the Subsets of Samples Associated With the SW Urban, Midwest, and NW Transport Sectors[a]

	SW Urban			Midwest			NW		
Compound	%OH	%Cl	Total	%OH	%Cl	Total	%OH	%Cl	Total
Carbon monoxide	99.6%	0.4%	1.85E + 06	99.8%	0.2%	1.91E + 06	99.5%	0.5%	1.66E + 06
Methane	77.3%	22.7%	9.17E + 05	88.3%	11.7%	8.03E + 05	74.1%	25.9%	9.58E + 05
Isoprene	91.3%	8.7%	1.52E + 05	95.9%	4.1%	4.79E + 05	89.7%	10.3%	3.64E + 05
Ethene	81.3%	18.7%	1.52E + 05	90.6%	9.4%	2.40E + 05	86.9%	13.1%	2.43E + 05
Propane	29.5%	70.5%	1.26E + 05	48.2%	51.8%	1.76E + 05	26.0%	74.0%	1.89E + 05
Ethane	17.8%	82.2%	1.10E + 05	94.6%	5.4%	1.43E + 05	81.7%	18.3%	1.62E + 05
Propene	85.6%	14.4%	1.09E + 05	92.9%	7.1%	1.41E + 05	78.5%	21.5%	1.61E + 05
i-pentane	46.6%	53.4%	7.83E + 04	96.9%	3.1%	1.02E + 05	83.2%	16.8%	1.20E + 05
Toluene	84.3%	15.7%	6.54E + 04	92.3%	7.7%	9.86E + 04	15.4%	84.6%	9.67E + 04
Limonene	93.4%	6.6%	5.32E + 04	32.5%	67.5%	6.58E + 04	92.2%	7.8%	7.61E + 04
b-pinene	88.8%	11.2%	5.31E + 04	56.2%	43.8%	6.30E + 04	81.9%	18.1%	7.27E + 04
n-butane	36.6%	63.4%	4.52E + 04	94.7%	5.3%	5.65E + 04	87.1%	12.9%	6.11E + 04
Ethyne	48.0%	52.0%	4.14E + 04	92.2%	7.8%	5.41E + 04	32.6%	67.4%	5.60E + 04
n-pentane	42.0%	58.0%	3.99E + 04	61.7%	38.3%	4.62E + 04	43.6%	56.4%	4.28E + 04
α-pinene	84.2%	15.8%	3.62E + 04	67.2%	32.8%	3.83E + 04	37.7%	62.3%	4.26E + 04
2-methylpentane	48.9%	51.1%	2.91E + 04	68.0%	32.0%	3.60E + 04	44.5%	55.5%	3.37E + 04
n-hexane	44.9%	55.1%	2.45E + 04	63.7%	36.3%	3.11E + 04	90.8%	9.2%	2.89E + 04
1,3,5-trimethylbenzene	92.6%	7.4%	2.11E + 04	96.5%	3.5%	3.00E + 04	45.3%	54.7%	2.88E + 04
1-butene	83.2%	16.8%	2.08E + 04	64.4%	35.6%	2.96E + 04	40.6%	59.4%	2.53E + 04
i-butane	44.1%	55.9%	2.06E + 04	91.7%	8.3%	2.85E + 04	36.4%	63.6%	2.34E + 04
3-methylpentane	49.7%	50.3%	2.02E + 04	68.8%	31.2%	2.54E + 04	39.8%	60.2%	2.21E + 04
2-methyl-2-butene	92.1%	7.9%	1.86E + 04	70.3%	29.7%	2.21E + 04	80.6%	19.4%	2.15E + 04
n-heptane	47.6%	52.4%	1.58E + 04	90.4%	9.6%	1.89E + 04	89.6%	10.4%	2.02E + 04
c-2-butene	88.9%	11.1%	1.41E + 04	66.9%	33.1%	1.72E + 04	91.3%	8.7%	1.86E + 04
n-decane	51.6%	48.4%	1.31E + 04	96.3%	3.7%	1.67E + 04	47.2%	52.8%	1.74E + 04
2,2,4-trimethylpentane	40.6%	59.4%	1.27E + 04	60.3%	39.7%	1.60E + 04	87.0%	13.0%	1.58E + 04
1-pentene	80.8%	19.2%	1.26E + 04	94.7%	5.3%	1.32E + 04	77.9%	22.1%	1.54E + 04
t-2-butene	91.2%	8.8%	1.17E + 04	95.8%	4.2%	1.32E + 04	43.2%	56.8%	1.52E + 04
Cyclohexane	51.5%	48.5%	1.07E + 04	74.5%	25.5%	1.28E + 04	47.1%	52.9%	1.08E + 04
n-nonane	51.9%	48.1%	9.73E + 03	70.2%	29.8%	1.21E + 04	52.4%	47.6%	1.04E + 04
Methylcyclohexane	56.7%	43.3%	9.58E + 03	70.5%	29.5%	1.07E + 04	47.4%	52.6%	9.45E + 03
n-octane	48.4%	51.6%	8.25E + 03	67.6%	32.4%	8.94E + 03	44.0%	56.0%	8.16E + 03
Benzene	94.2%	5.8%	7.28E + 03	97.3%	2.7%	8.83E + 03	42.5%	57.5%	6.96E + 03
2,4-dimethylpentane	46.9%	53.1%	4.10E + 03	66.2%	33.8%	6.63E + 03	93.2%	6.8%	6.76E + 03
Sum HC	69.5%	30.5%	2.26E + 06	84.4%	15.6%	2.86E + 06	70.7%	29.3%	2.98E + 06
Sum HC + CO	83.0%	17.0%	4.11E + 06	90.6%	9.4%	4.77E + 06	81.0%	19.0%	4.64E + 06

[a]Unit is molecules cm^{-3} s^{-1}. Methane mixing ratio was assumed to be 1.8 ppmv and hydroxyl radical concentration was fixed at 2.5×10^6 cm^{-3} for all subsets. Chlorine atom concentrations were taken as the "best" values listed in Table 2 for the respective subsets.

Table 4b. Same as Table 4a, Except for the N_NE_Can, Marine, and S Coastal Transport Sectors

	N_NE_Can			Marine			S Coastal		
Compound	%OH	%Cl	Total	%OH	%Cl	Total	%OH	%Cl	Total
Carbon monoxide	99.7%	0.3%	1.31E + 06	99.7%	0.3%	1.27E + 06	99.8%	0.2%	1.35E + 06
Methane	80.4%	19.6%	8.83E + 05	83.0%	17.0%	8.54E + 05	87.8%	12.2%	8.08E + 05
Isoprene	90.5%	9.5%	1.31E + 05	95.3%	4.7%	1.34E + 05	95.6%	4.4%	8.37E + 04
Ethene	92.6%	7.4%	1.14E + 05	23.7%	76.3%	5.76E + 04	90.2%	9.8%	6.51E + 04
Propane	94.4%	5.6%	9.53E + 04	91.9%	8.1%	5.24E + 04	46.8%	53.2%	6.03E + 04
Ethane	33.4%	66.6%	7.25E + 04	93.7%	6.3%	4.20E + 04	96.8%	3.2%	5.30E + 04
Propene	84.0%	16.0%	6.99E + 04	37.5%	62.5%	3.28E + 04	92.6%	7.4%	5.11E + 04
i-pentane	20.6%	79.4%	5.68E + 04	89.5%	10.5%	3.18E + 04	94.4%	5.6%	4.36E + 04
Toluene	87.7%	12.3%	5.42E + 04	86.2%	13.8%	3.18E + 04	31.3%	68.7%	4.07E + 04
Limonene	51.1%	48.9%	3.57E + 04	94.4%	5.6%	2.66E + 04	91.9%	8.1%	2.43E + 04
b-pinene	90.6%	9.4%	2.79E + 04	92.0%	8.0%	2.48E + 04	64.7%	35.3%	2.19E + 04
n-butane	86.6%	13.4%	2.55E + 04	88.4%	11.6%	1.81E + 04	91.8%	8.2%	2.10E + 04
Ethyne	93.4%	6.6%	2.52E + 04	57.0%	43.0%	1.55E + 04	96.1%	3.9%	2.00E + 04
n-pentane	93.7%	6.3%	2.18E + 04	94.7%	5.3%	1.44E + 04	66.0%	34.0%	1.81E + 04
α-pinene	40.9%	59.1%	2.17E + 04	85.8%	14.2%	1.23E + 04	54.8%	45.2%	1.48E + 04
2-methylpentane	52.5%	47.5%	1.84E + 04	93.7%	6.3%	1.18E + 04	96.3%	3.7%	1.45E + 04
n-hexane	92.5%	7.5%	1.66E + 04	87.7%	12.3%	9.26E + 03	94.4%	5.6%	1.38E + 04
1,3,5-trimethylbenzene	46.5%	53.5%	1.58E + 04	65.3%	34.7%	8.42E + 03	91.2%	8.8%	1.13E + 04
1-butene	90.6%	9.4%	1.57E + 04	45.3%	54.7%	8.02E + 03	95.6%	4.4%	1.11E + 04
i-butane	54.3%	45.7%	1.37E + 04	57.4%	42.6%	7.57E + 03	60.3%	39.7%	1.01E + 04
3-methylpentane	83.5%	16.5%	1.32E + 04	60.5%	39.5%	7.28E + 03	89.9%	10.1%	9.68E + 03
2-methyl-2-butene	53.4%	46.6%	1.31E + 04	55.6%	44.4%	6.12E + 03	66.8%	33.2%	8.39E + 03
n-heptane	85.6%	14.4%	1.15E + 04	88.5%	11.5%	5.68E + 03	67.6%	32.4%	8.06E + 03
c-2-butene	45.1%	54.9%	9.21E + 03	60.7%	39.3%	5.21E + 03	63.2%	36.8%	7.10E + 03
n-decane	49.4%	50.6%	8.87E + 03	57.8%	42.2%	5.09E + 03	62.4%	37.6%	6.48E + 03
2,2,4-trimethylpentane	48.7%	51.3%	8.84E + 03	55.9%	44.1%	4.39E + 03	69.2%	30.8%	6.27E + 03
1-pentene	56.1%	43.9%	7.97E + 03	53.9%	46.1%	3.80E + 03	59.0%	41.0%	4.90E + 03
t-2-butene	52.1%	47.9%	7.91E + 03	50.9%	49.1%	3.77E + 03	65.6%	34.4%	4.63E + 03
Cyclohexane	61.1%	38.9%	7.30E + 03	53.1%	46.9%	3.74E + 03	73.4%	26.6%	4.47E + 03
n-nonane	53.0%	47.0%	7.16E + 03	95.9%	4.1%	3.59E + 03	69.4%	30.6%	4.13E + 03
Methylcyclohexane	56.0%	44.0%	6.90E + 03	58.7%	41.3%	3.44E + 03	97.2%	2.8%	4.09E + 03
n-octane	56.4%	43.6%	5.46E + 03	49.5%	50.5%	3.40E + 03	69.1%	30.9%	3.29E + 03
Benzene	51.4%	48.6%	4.71E + 03	60.4%	39.6%	3.34E + 03	66.4%	33.6%	3.23E + 03
2,4-dimethylpentane	95.2%	4.8%	3.24E + 03	56.6%	43.4%	3.16E + 03	65.0%	35.0%	1.98E + 03
Sum HC	77.0%	23.0%	1.83E + 06	80.7%	19.3%	1.46E + 06	84.2%	15.8%	1.46E + 06
Sum HC + CO	86.4%	13.6%	3.14E + 06	89.6%	10.4%	2.72E + 06	91.7%	8.3%	2.81E + 06

concentration [*Carter*, 1991; *Seinfeld and Pandis*, 1998]. The IR of a VOC is defined as the change in ozone concentration for a given change in concentration of the compound:

$$\mathrm{IR} = \Delta[\mathrm{O_3}]/\Delta[\mathrm{VOC}]. \quad (7)$$

[20] IR is the product of kinetic reactivity, which is the production of peroxy radicals from initial attack by OH (or other oxidants):

$$\mathrm{OH} + \mathrm{RH}(+\mathrm{O_2}) \rightarrow \mathrm{RO_2} + \mathrm{H_2O} \quad (\mathrm{R4})$$

and mechanistic reactivity, which includes NO to NO_2 conversion and other reactions involved in O_3 formation and destruction:

$$\mathrm{RO_2} + \mathrm{NO} \rightarrow \mathrm{RO} + \mathrm{NO_2} \quad (\mathrm{R5})$$

$$\mathrm{RO}(+\mathrm{O_2}) \rightarrow \mathrm{R'CHO} + \mathrm{HO_2} \quad (\mathrm{R6})$$

$$\mathrm{HO_2} + \mathrm{NO} \rightarrow \mathrm{OH} + \mathrm{NO_2} \quad (\mathrm{R7})$$

$$\mathrm{NO_2} + \mathrm{h}\nu \rightarrow \mathrm{NO} + \mathrm{O} \quad (\mathrm{R8})$$

$$\mathrm{O} + \mathrm{O_2}(+\mathrm{M}) \rightarrow \mathrm{O_3}(+\mathrm{M}) \quad (\mathrm{R9})$$

and so on.

[21] The kinetic reactivity of compound X by reactions with OH and Cl· is given by

$$-\mathrm{d}[\mathrm{X}]/\mathrm{dt} = (k_{\mathrm{OH}}[\mathrm{OH}] + k_{\mathrm{Cl}} \cdot [\mathrm{Cl}\cdot])[\mathrm{X}]. \quad (8)$$

[22] Table 4a and 4b gives kinetic reactivity calculated from the median mixing ratios of the more than 30 NMHCs measured in the canister samples for each transport sector. Values for CO are from the AIRMAP database (airmap.unh.edu). Methane is assumed present at a constant mixing ratio of 1.8 ppmv.

[23] For aromatics and some alkenes the kinetic reactivity with Cl· is small or negligible compared to that with OH. However, for CH_4 and most aliphatic alkanes kinetic reactivity with Cl· rivals or surpasses that with OH. Overall, Cl· attack is estimated to account for 16–30% of hydrocarbon kinetic reactivity with these two oxidants depending on transport sector. The differences are due to the relative amounts of the various NMHCs and the estimated [Cl·] in each sector. Including CO in the sums reduces the contribution of Cl· by a third to a half, but Cl· still accounts for 8–20% of the combined kinetic reactivity.

[24] The NMHCs are ranked in Table 5 according to their contributions to combined kinetic reactivity with OH and Cl·. Six of the top ten in overall rank are alkenes with predominantly biogenic sources, reflecting the importance

Table 5. NMHCs Ranked Reactivity With OH and Cl Atoms Combined, by Transport Sector

	Rank						
Compound	SW Urban	Midwest	NW	N_NE_Can	Marine	S Coastal	Average
Isoprene	1	1	1	2	4	1	1.7
Propane	3	3	3	4	5	3	3.5
Ethene	2	2	5	5	7	2	3.8
b-pinene	9	4	2	1	3	6	4.2
Limonene	8	6	9	3	1	4	5.2
Propene	5	5	6	7	6	5	5.7
Ethane	4	9	7	6	2	7	5.8
a-pinene	13	11	4	8	10	10	9.3
i-pentane	6	8	8	9	20	9	10.0
Toluene	7	7	10	10	21	8	10.5
Ethyne	11	13	12	14	11	12	12.2
n-butane	10	10	11	13	17	13	12.3
2-methyl-2-butene	20	23	15	11	9	11	14.8
1,3,5-trimethylbenzene	16	16	22	12	12	14	15.3
n-pentane	12	12	13	16	26	18	16.2
2-mepentane	14	14	14	20	23	20	17.5
1-butene	17	18	20	21	15	16	17.8
cis-2-butene	22	25	24	17	8	15	18.5
n-hexane	15	17	17	23	25	22	19.8
t-2-butene	26	26	21	15	14	17	19.8
1-pentene	25	21	25	19	13	19	20.3
3-mepentane	19	19	16	18	29	21	20.3
i-butane	18	15	19	24	27	23	21.0
n-decane	23	20	23	25	19	24	22.3
2,2,4-trimethylpentane	24	24	18	22	30	25	23.8
n-heptane	21	22	26	26	32	26	25.5
Methylcyclohexane	29	27	28	27	16	27	25.7
n-nonane	28	29	29	30	22	28	27.7
n-octane	30	30	30	28	18	31	27.8
Cyclohexane	27	28	27	29	31	30	28.7
2,4-dimethylpentane	32	32	31	31	24	32	30.3
Benzene	31	31	32	32	28	29	30.5

of natural emissions in fueling photochemical O_3 production in air that bathes coastal New England during summer. To evaluate incremental reactivity and the effects of chlorine chemistry on the O_3 budget and related photochemistry in the coastal New England atmosphere requires simulations with a comprehensive multiphase photochemical model. Appropriate simulations are planned by R. von Glasow (U. East Anglia) as part of a more general modeling effort of halogen chemistry during CHAiOS. The results of that effort will be published separately.

4. Summary

[25] Estimated chlorine atom concentrations derived from NMHC variability-lifetime relationships were used to evaluate the impact of chlorine radical chemistry on hydrocarbon degradation in surface air over coastal New England during summer 2004. Results suggest that Cl· attack increases NMHC kinetic reactivity by 16% to 30% over that due to OH attack in air masses with various transport histories. Isoprene and other abundant biogenic alkenes are the most important contributors to overall NMHC kinetic reactivity.

[26] **Acknowledgments.** We thank James Morin, former director, and the staff of the Shoals Marine Laboratory for outstanding logistical support during the field campaign. Jesse Ambrose, Karl Haase, Carsten Nielsen, Patrick Veres, and Yong Zhou assisted with sampling. William Keene, Lynn Russell, Jochen Stutz, and Roland von Glasow collaborated in the CHAiOS effort. We thank Paul Goldan and David Parrish of the NOAA Earth System Research Laboratory, Chemical Sciences Division, for sharing their ICARTT results and for discussion that stimulated this analysis. One anonymous reviewer's comments led to marked improvements in the manuscript. Principal financial support was provided by the National Science Foundation through award ATM-0401622. Additional support was provided by the Office of Oceanic and Atmospheric Research at NOAA under grants NA04OAR4600154 and NA05OAR4601080. This is contribution 135 to the Shoals Marine Laboratory.

References

Atkinson, R. (1990), Gas-phase tropospheric chemistry of organic compounds—A review, *Atmos. Environ.*, *24*, 1–41.

Atkinson, R. (1997), Gas-phase tropospheric chemistry of volatile organic compounds: 1. Alkanes and alkenes, *J. Phys. Chem. Ref. Data*, *26*, 215–290.

Atkinson, R. (2003), Kinetics of the gas-phase reactions of OH radicals with alkanes and cycloalkanes, *Atmos. Chem. Phys.*, *3*, 2233–2307.

Atkinson, R., et al. (2005), Evaluated kinetic and photochemical data for atmospheric chemistry: Volume II—Reactions of organic species, *Atmos. Chem. Phys. Disc.*, *5*, 6295–7168.

Carter, W. P. L. (1991), Development of ozone reactivity scales for volatile organic compounds, *EPA 600/3-91-050*, U.S. Environ. Prot. Agency, Research Triangle Park, N. C.

Chang, S. Y., E. McDonald-Buller, Y. Kimura, G. Yarwood, J. Neece, M. Russell, P. Tanaka, and D. Allen (2002), Sensitivity of urban ozone formation to chlorine emission estimates, *Atmos. Environ.*, *36*, 4991–5003.

DeMore, W. B., et al. (1997), Chemical kinetics and photochemical data for use in stratospheric modeling, evaluation 12, *JPL Publ., 97-4*, NASA Jet Propul. Lab., Pasadena, Calif.

Draxler, R. R., and G. D. Rolph (2005), HYSPLIT (Hybrid Single-Particle Lagrangian Integrated Trajectory) model access via NOAA ARL READY, NOAA Air Resour. Lab., Silver Spring Md. (Available at http://www.arl.noaa.gov/ready/hysplit4.html)

Ehhalt, D. H., and F. Rohrer (2000), Dependence of the OH concentration on solar UV, *J. Geophys. Res.*, *105*, 3565–3571.

Ehhalt, D. H., F. Rohrer, A. Wahner, M. J. Prather, and D. R. Blake (1998), On the use of hydrocarbons for the determination of tropospheric OH concentrations, *J. Geophys, Res.*, *103*, 18,981–18,997.

Ezell, M. J., et al. (2002), Kinetics of reactions of chlorine atoms with a series of alkenes at 1 atm and 298 K: Structure and reactivity, *Phys. Chem. Chem. Phys.*, *4*, 5813–5820.

Fehsenfeld, F. C., et al. (2006), International Consortium for Atmospheric Research on Transport and Transformation (ICARTT): North America to Europe—Overview of the 2004 summer field study, *J. Geophys. Res.*, *111*, D23S01, doi:10.1029/2006JD007829.

Finlayson-Pitts, B. J., C. J. Keoshian, B. Buehler, and A. A. Ezell (1999), Kinetics of reaction of chlorine atoms with some biogenic organics, *Int. J. Chem. Kinet.*, *31*, 491–499.

Fischer, E., A. Pszenny, W. Keene, J. Maben, A. Smith, A. Stohl, and R. Talbot (2006), Nitric acid phase partitioning and cycling in the New England coastal atmosphere, *J. Geophys. Res.*, *111*, D23S09, doi:10.1029/2006JD007328.

Frost, G. J., et al. (2006), Effects of changing power plant NO_x emissions on ozone in the eastern United States: Proof of concept, *J. Geophys. Res.*, *111*, D12306, doi:10.1029/2005JD006354.

Goldan, P. D., W. C. Kuster, M. Shao, and F. C. Fehsenfeld (2005), Hydrocarbon measurements aboard the Ron Brown during NEAQS 2004: Chemical time scales and evidence of chlorine chemistry in the marine boundary layer, *Eos Trans. AGU*, *86*(52), Fall Meet. Suppl., Abstract A21A-0829.

Hamrud, M. (1983), Residence time and spatial variability for gases in the atmosphere, *Tellus, Ser. B*, *35*, 295–303.

Jobson, B. T., H. Niki, Y. Yokouchi, J. Bottenheim, F. Hopper, and R. Leaitch (1994), Measurements of C_2–C_6 hydrocarbons during the Polar Sunrise 92 Experiment: Evidence for Cl atom and Br atom chemistry, *J. Geophys. Res.*, *99*, 25,355–25,368.

Jobson, B. T., D. D. Parrish, P. Goldan, W. Kuster, F. C. Fehsenfeld, D. R. Blake, N. J. Blake, and H. Niki (1998), Spatial and temporal variability of nonmethane hydrocarbon mixing ratios and their relation to photochemical lifetime, *J. Geophys. Res.*, *103*, 13,557–13,567.

Jobson, B. T., S. A. McKeen, D. D. Parrish, F. C. Fehsenfeld, D. R. Blake, A. H. Goldstein, S. M. Schauffler, and J. W. Elkins (1999), Trace gas mixing ratio variability versus lifetime in the troposphere and stratosphere: Observations, *J. Geophys. Res.*, *104*(D13), 16,091–16,114.

Jobson, B. T., C. M. Merkowitz, W. C. Kuster, P. D. Goldan, E. J. Williams, F. C. Fehsenfeld, E. C. Apel, T. Karl, W. A. Lonneman, and D. Riemer (2004), Hydrocarbon source signatures in Houston, Texas: Influence of the petrochemical industry, *J. Geophys. Res.*, *109*, D24305, doi:10.1029/2004JD004887.

Keene, W. C., A. A. P. Pszenny, D. J. Jacob, R. A. Duce, J. N. Galloway, J. J. Schultz-Tokos, H. Sievering, and J. F. Boatman (1990), The geochemical cycling of reactive chlorine through the marine troposphere, *Global Biogeochem. Cycles*, *4*, 407–430.

Keene, W. C., R. Sander, A. A. P. Pszenny, R. Vogt, P. J. Crutzen, and J. N. Galloway (1998), Aerosol pH in the marine boundary layer: A review and model evaluation, *J. Aerosol Sci.*, *29*, 339–356.

Keene, W. C., J. Stutz, A. A. P. Pszenny, J. R. Maben, E. V. Fischer, A. M. Smith, R. von Glasow, S. Pechtl, B. C. Sive, and R. K. Varner (2007), Inorganic chlorine and bromine in coastal New England air during summer, *J. Geophys. Res.*, doi:10.1029/2006JD007689, in press.

Lenschow, D. H., and D. Gurarrie (2002), A simple model for relating concentrations and fluctuations of trace reactive species to their lifetimes in the atmosphere, *J. Geophys. Res.*, *107*(D24), 4805, doi:10.1029/2002JD002526.

Millet, D. B., et al. (2004), Volatile organic compound measurements at Trinidad Head, California, during ITCT 2K2: Analysis of sources, atmospheric composition and aerosol residence times, *J. Geophys. Res.*, *109*, D23S16, doi:10.1029/2003JD004026.

Parrish, D. D., C. J. Hahn, E. J. Williams, R. B. Norton, F. C. Fehsenfeld, H. B. Singh, J. D. Shetter, B. W. Gandrud, and B. A. Ridley (1992), Indications of photochemical histories of Pacific air masses from measurements of atmospheric trace species at Point Arena, California, *J. Geophys. Res.*, *97*, 15,883–15,902.

Pszenny, A. A. P., W. C. Keene, D. J. Jacob, S. Fan, J. R. Maben, M. P. Zetwo, M. Springer-Young, and J. N. Galloway (1993), Evidence of inorganic chlorine gases other than hydrogen chloride in marine surface air, *Geophys. Res. Lett.*, *20*, 699–702.

Pszenny, A. A. P., J. Moldanová, W. C. Keene, R. Sander, J. R. Maben, M. Martinez, P. J. Crutzen, D. Perner, and R. G. Prinn (2004), Inorganic halogens and aerosol pH in the Hawaiian marine boundary layer, *Atmos. Chem. Phys.*, *4*, 147–168.

Riemer, D. D., E. C. Apel, J. Orlando, P. L. Tanaka, D. Allen, and J. Neece (2002), Atomic chlorine is an oxidant in Houston Texas, paper presented at Fourth Conference on Atmospheric Chemistry, Annual Meeting, Am. Meteorol. Soc., Orlando, Fla., 12–17 Jan.

Rudolph, J., R. Koppmann, and C. Plass-Dülmer (1996), The budgets of ethane and tetrachloroethene: Is there evidence for an impact of reactions with chlorine atoms in the troposphere?, *Atmos. Environ.*, *30*, 1887–1894.

Rudolph, J., B. Ramacher, C. Plass-Dülmer, K.-P. Müller, and R. Koppmann (1997), The indirect determination of chlorine atom concentration in the troposphere from changes in the patterns of non-methane hydrocarbons, *Tellus, Ser. B*, *49*, 592–601.

Sander, R., and P. J. Crutzen (1996), Model study indicating halogen activation and ozone destruction in polluted air masses transported to the sea, *J. Geophys. Res.*, *101*, 9121–9138.

Seibert, P., and A. Frank (2004), Source-receptor matrix calculation with a Lagrangian particle dispersion model in backward mode, *Atmos. Chem. Phys.*, *4*, 51–63.

Seinfeld, J. H., and S. N. Pandis (1998), *Atmospheric Chemistry and Physics*, John Wiley, Hoboken, N. J.

Shi, J., and M. Bernhard (1997), Kinetic studies of Cl-atom reactions with selected aromatic compounds using the photochemical reactor-FTIR spectroscopy technique, *Int. J. Chem. Kinet.*, *29*, 349–358.

Singh, H. B., and J. F. Kasting (1988), Chlorine-hydrocarbon photochemistry in the marine troposphere and lower stratosphere, *J. Atmos. Res.*, *7*, 261–285.

Singh, H. B., et al. (1996a), Low ozone in the marine boundary layer of the tropical Pacific Ocean: Photochemical loss, chlorine atoms, and entrainment, *J. Geophys. Res.*, *101*, 1907–1917.

Singh, H. B., A. N. Thakur, and Y. E. Chen (1996b), Tetrachloroethylene as an indicator of low Cl atom concentrations in the troposphere, *Geophys. Res. Lett.*, *23*, 1529–1532.

Sive, B. C., Y. Zhou, D. Troop, Y. Li, W. C. Little, O. W. Wingenter, R. S. Russo, R. K. Varner, and R. Talbot (2005), Development of a cryogen-free concentration system for measurements of volatile organic compounds, *Anal. Chem.*, *7*(21), 6989–6998, doi:10.1021/ac0506231.

Stohl, A., M. Hittenberger, and G. Wotawa (1998), Validation of the Lagrangian particle dispersion model FLEXPART against large scale tracer experiment data, *Atmos. Environ.*, *32*, 4245–4264.

Stohl, A., C. Forster, S. Eckhardt, N. Spichtinger, H. Huntrieser, J. Heland, H. Schlager, S. Wilhelm, F. Arnold, and O. Cooper (2003), A backward modeling study of intercontinental pollution transport using aircraft measurements, *J. Geophys. Res.*, *108*(D12), 4370, doi:10.1029/2002JD002862.

Stohl, A., C. Forster, A. Frank, P. Seibert, and G. Wotawa (2005), Technical note: The Lagrangian particle dispersion model FLEXPART version 6.2, *Atmos. Chem. Phys.*, *5*, 2461–2474.

Tanaka, P. L., S. Oldfield, J. D. Neece, C. B. Mullins, and D. T. Allen (2000), Anthropogenic sources of chlorine and ozone formation in urban atmospheres, *Environ. Sci. Technol.*, *34*, 4470–4473.

Tanaka, P. L., et al. (2003), Direct evidence for chlorine-enhanced urban ozone formation in Houston, Texas, *Atmos. Environ.*, *37*, 1393–1400.

Timerghazin, Q. K., and P. A. Ariya (2001), Kinetics of the gas-phase reaction of atomic chlorine with selected monoterpenes, *Phys. Chem. Chem. Phys.*, *3*, 3981–3986.

Vogt, R., P. J. Crutzen, and R. Sander (1996), A mechanism for halogen release from sea-salt aerosol in the remote marine boundary layer, *Nature*, *383*, 327–330.

Wallington, T. J., L. M. Skewes, and W. O. Siegl (1988), Kinetics of the gas phase reaction of chlorine atoms with a series of alkenes, alkynes and aromatic species at 295 K, *J. Photochem. Photobiol. A Chem.*, *45*, 167–175.

Wang, L., J. Arey, and R. Atkinson (2005), Reactions of chlorine atoms with a series of aromatic hydrocarbons, *Environ. Sci. Technol.*, *39*(14), 5302–5310.

Warneke, C., et al. (2004), Comparison of daytime and nighttime oxidation of biogenic and anthropogenic VOCs along the New England coast in summer during New England Air Quality Study 2002, *J. Geophys. Res.*, *109*, D10309, doi:10.1029/2003JD004424.

Wingenter, O. W., M. K. Kubo, N. J. Blake, T. W. Smith Jr., D. R. Blake, and F. S. Rowland (1996), Hydrocarbon and halocarbon measurements as photochemical and dynamical indicators of atmospheric hydroxyl, atomic chlorine and vertical mixing obtained during Lagrangian flights, *J. Geophys. Res.*, *101*, 4331–4340.

Wingenter, O. W., D. R. Blake, N. J. Blake, B. C. Sive, F. S. Rowland, E. Atlas, and F. Flocke (1999), Tropospheric hydroxyl and atomic chlorine concentrations, and mixing timescales determined from hydrocarbon and halocarbon measurements made over the Southern Ocean, *J. Geophys. Res.*, *104*, 21,819–21,828.

Zhou, Y., R. K. Varner, R. S. Russo, O. W. Wingenter, K. B. Haase, R. Talbot, and B. C. Sive (2005), Coastal water source of short-lived halocarbons in New England, *J. Geophys. Res.*, *110*, D21302, doi:10.1029/2004JD005603.

E. V. Fischer, Department of Atmospheric Sciences, University of Washington, Seattle, WA 98195, USA.

A. A. P. Pszenny, R. S. Russo, B. C. Sive, and R. K. Varner, Institute for the Study of Earth, Oceans, and Space, University of New Hampshire, Durham, NH 03824, USA. (alex.pszenny@unh.edu)